IEEE Access
Multidisciplinary | Rapid Review | Open Access Journal

Received March 9, 2018, accepted April 8, 2018, date of publication April 24, 2018, date of current version May 24, 2018.

Digital Object Identifier 10.1109/ACCESS.2018.2829731

Space-Frequency Modulation Radar-Communication and Mismatched Filtering

ZHAOFENG WANG, GUISHENG LIAO, (Senior Member, IEEE), AND ZHIWEI YANG
National Laboratory of Radar Signal Processing, Xidian University, Xi'an 710071, China

Corresponding author: Zhaofeng Wang (wzf_0507@126.com)

This work was supported by the National Natural Science Foundation of China under Grant 61671352 and Grant 61231017.

ABSTRACT Increasing congestion has spurred investigations into more efficient utilization of the radio frequency (RF) spectrum while minimizing the volume and weight of the RF equipment. Considering the similarity of radar and communication in both software and hardware, this paper presents a co-design integrated waveform of radar and communication based on the multiantenna system. In this paper, communication data is first transported by utilizing space-frequency modulation on a fixed transmitting frequency set. By using digital beamforming technology in the subarray level, directional communication with cooperative targets in the main lobe can be achieved. However, modulation in space-frequency domain results in high sidelobes in the autocorrelation function. Thus, to acquire an acceptable radar performance, the mismatched filter (MMF) is proposed to realize information defusion and sidelobe suppression. Aiming at reducing the signal-to-noise ratio loss of the MMF process, the filter response is further modified. Finally, numerical simulations assess the effectiveness of the proposed MMF and the Doppler coherency between pulses for clutter cancellation. Simulation results demonstrate the capability and potential of the proposed co-design signal for radar-communication system.

INDEX TERMS Radar-communication, waveform design, mismatched filter, space-frequency modulation.

I. INTRODUCTION

The increasing number of wireless devices and the growing bandwidth needs caused by high speed data transfer requirements have led to overcrowding in the electromagnetic spectrum. For emerging unmanned platforms, such as unmanned aerial vehicles (UAVs) and unmanned ship vehicles (USVs), the limited capacity of volume and load also conflict with the diversified devices required.

In the field of multifunction radio frequency (RF) systems, the research on an integration system of radar and communication has drawn great attention because of the advantages of efficiently alleviating electromagnetic interference, lowering the radar cross section (RCS) and reducing the costs [1]. Moreover, the fusion of radar and communication has the potential of mutual enhancement. For example, the high efficiency power amplifier and directivity radiation of radar increase the maximum range of communication and improve information security, respectively, in some military applications. Furthermore, communication data modulation introduces a difference of the emitting waveform between pulses or coherence process intervals (CPIs). This modulation may enable more degrees of freedom (DoFs) in time for the radar function, if properly used. In the worldwide communication protocol IEEE802.11a [2], additional pieces, such as the physical layer convergence protocol (PLCP) preamble, are supposed to achieve timing synchronization and frequency offset estimation, which are similar to the estimations of range and Doppler in radar. Hence, for the purpose of increasing the utilization of system resources, the fusion of radar and communication in the transmitting signal is feasible and necessary.

Much work has been done to achieve an integrated system of radar and communication through designing a unified signal frame. One of the most critical issues to be considered is the method to realize signals or information fusion. A straightforward method to obtain the integration signal is to make the signals of two functions separable in some domain. For example, information transmission and radar sensing could be functioning separately in the time domain [3] or the frequency domain [4]. Moreover, different methods to acquire the orthogonality in other domains have been considered, such as using opposite chirp slopes [5], [6]

and orthogonal spread-spectrum sequence [7], [8]. Alternatively, in [9], the communication data is modulated onto the linear frequency modulation (LFM) signal in an insensitive level for radar function, and the modulation effect on radar operation is ignored. As has been widely used in the digital broadcasting and wireless local area network (WLAN) for communication application, the OFDM waveform draws attention in the area of radar signal processing recently. The OFDM signal as a radar waveform has been developed in several works with respect to space time adaptive processing (STAP) [10], synthetic aperture radar (SAR) imaging [11], target detection [12], etc. For the application of integrated radar and communication system, in [13]–[15], the phase modulated OFDM signal is transmitted directly in a communication system. Thus, the communication information is removed from the received signal before the radar operation. However, although the OFDM signal has been exploited deeply in commercial communication and shows potential for radar application gradually, the high peak to average power ratio (PAPR) of OFDM will cause distortion through the nonlinear amplifier that commonly applied in radar system.

With the development of antenna technology, array antenna is becoming increasingly common in military radar system. Similarly, in communication, recently proposed multiple-input multiple-output (MIMO) antenna systems [16] or space-division multiplexing (SDM) systems are further revolutionizing antenna systems for wireless communications. With the intention of exploring the information carry capability in the spatial domain, we focus on the waveform design based on a multi-antenna system and first introduced the space-frequency modulation (SFM) waveform in [17]. In the proposed SFM waveform, communication data is first transported by utilizing space-frequency modulation on a fixed antenna array. By using digital beamforming (DBF) technology in the sub-array level, directional communication with the cooperative target in the main lobe can be achieved. However, the issue with this modulated waveform is the high sidelobes in the autocorrelation function (ACF) caused by spectrum modulation. Inspired by the element-wise division in [15], the transmitted information is employed as prior knowledge to construct the corresponding mismatched filter (MMF). Finally, after information defusion before radar operation, the sidelobes are well suppressed at the cost of an acceptable loss of processing signal to noise ratio (SNR).

The major contributions in this paper are threefold: 1) to propose an integrated waveform of radar and communication utilizing space-frequency modulation based on multi-antenna system, 2) to analyze the effect of data modulation on the radar performance by deriving the ACF, and 3) to propose the MMF to complete information defusion and suppress the pulse compression (PC) sidelobes for the radar function.

The rest of this paper is organized as follows. In Section II, the SFM signal model is introduced including the primary signal model, modulation principle and the drawback of ACF needs to be regarded. Section III proposes the MMF derivation and further modification for lower SNR loss. Numerical simulation experiments are provided in Section IV followed by conclusions in Section V.

II. SPACE-FREQUENCY MODULATION SIGNAL

The operating procedure of the proposed integrated system can be briefly described in Fig. 1. First, the integrated waveform is generated through SFM on the primary signal. Next, the DBF technology is employed to form directional beams both for radar function and communication function. The transmit signal is capable of delivering communication data to the cooperate object while continuously detecting the interesting space in the same direction simultaneously. One potential application for the proposed waveform is the guidance system for missiles or other unmanned equipment. The detection result, including distance, azimuth and velocity, will be obtained from the radar processing. For the communication receiver, the modulated data will be extracted from the received signal through joint demodulation with amplitude and frequency.

A. PRIMARY SIGNAL MODEL

Consider the transmitting antenna as a uniform linear array with N_a elements. For N_a transmit antennas, in each pulse, there are N frequencies available to choose. The N_t frequencies finally transmitted by N_a antennas are obtained by SFM on the transmit frequency set $\boldsymbol{F}_{\mathbf{set}}$. At the receiver, by identifying N_t frequencies transmitted and analyzing

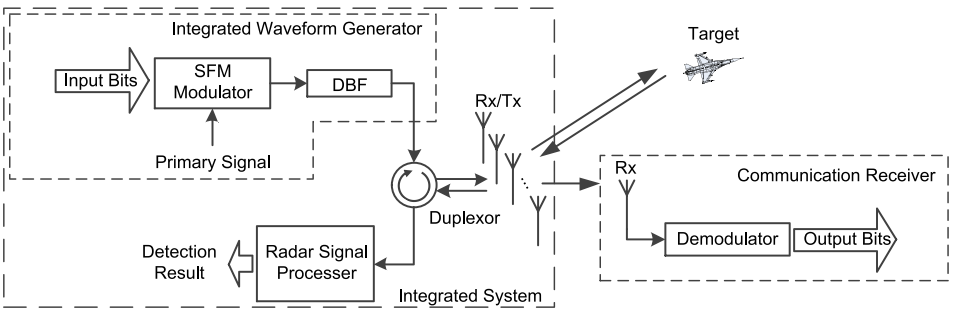

FIGURE 1. Operation procedure of the proposed integrated system.

their relative powers, the SFM matrix can be recovered to realize information demodulation. In the time domain, the proposed signal employs multiple sub-chips in one transmit pulse to increase the communication data rate. Alternatively, the incomplete and non-uniform transmitting signal spectrum caused by random modulation can be relieved by synthesis of multiple sub-chips. Consequently, the point spread function (PSF) deteriorations e.g. range resolution, range sidelobe are supposed to be relieved. The structure of the transmit signal is shown in Fig. 2. For convenience, the transmitting signal of each antenna is assumed to be a single frequency signal. In the k-th sub-chip, the transmit signal from the n_ath antenna can be written as

$$s_{n_a,k}(t) = \text{rect}\left(\left(t-(k-1)T_s\right)/T_s\right)\exp\left\{j2\pi\left(f_{n_a,k}+f_c\right)t\right\} \tag{1}$$

where

$$\text{rect}(x) = \begin{cases} 1, & 0 \le x < 1 \\ 0, & \text{else} \end{cases}$$

$k = 1, 2, \ldots, K$ represents sub-chip index, and $n_a = 1, 2, \ldots, N$ is the antenna index. The variable $f_{n_a,k}$ represents the signal frequency transmitted from antenna n_a, in the k-th sub-chip. The carrier frequency is f_c and the time width of each sub-chip is T_s.

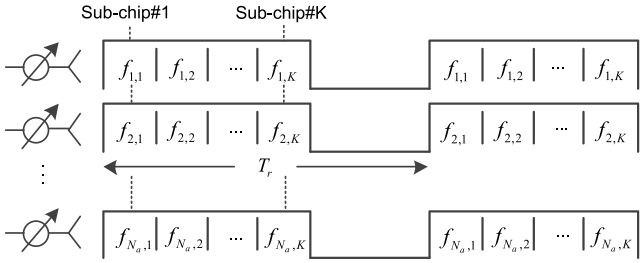

FIGURE 2. Sketch map of transmit signal.

B. MODULATION PRINCIPLE

The frequencies of the N_a transmit antenna in K sub-chips can be written in matrix form:

$$\boldsymbol{F} = [\boldsymbol{F}_1, \boldsymbol{F}_2, \cdots, \boldsymbol{F}_K] \tag{2}$$

where $\boldsymbol{F}_k \in \mathbb{Z}^{N_a \times 1}$, and $\boldsymbol{F}_k = \{f_{k,1}, f_{k,2}, \cdots f_{k,N_a}\}^{\mathrm{T}}$ represents the transmitting frequencies of each antenna in the *kth* sub-chip after space-frequency modulation, which is denoted as:

$$\boldsymbol{F}_k = \boldsymbol{C}_k \boldsymbol{F}_{\mathbf{set}} \tag{3}$$

with the transmit frequency set $\boldsymbol{F}_{\mathbf{set}} \in \mathbb{Z}^{N \times 1}$ and space-frequency modulation matrix $\boldsymbol{C}_k \in \mathbb{Z}^{N_a \times N}$.

$\boldsymbol{F}_{\mathbf{set}} = \{f_1, f_2, \cdots f_N\}^{\mathrm{T}}$ is an equally spaced frequency vector with its element

$$f_n = f_1 + (n-1)\Delta f_s. \tag{4}$$

Δf_s represents the step interval in the spatial domain, satisfying

$$\Delta f_s = 1/T_s, B = N\Delta f \ll f_c. \tag{5}$$

Considering that the communication receiver has no capability of determining the specific position of transmit antennas that share the same frequency, there are only two features that can be obtained: 1) the frequency set of transmitted signals from N_a antennas in one sub-chip; 2) the relative power between different frequencies on account of different numbers of transmitting antennas.

Consequently to ensure that $\boldsymbol{C}_k$ can be recovered from the received signal correctly and uniquely, several modulation principles are designed to guarantee the uniqueness of the demodulator outputs. The design of $\boldsymbol{C}_k$ should be restricted to the two rules given as follows:

Let $c_{i,j} = 0 \ or \ 1, \ i = 1, 2, \ldots, N_a, j = 1, 2, \ldots, N$ denotes the elements in $\boldsymbol{C}_k$ and $p, q \in \{1, 2, \ldots, N\}$.

(1) if $c_{i,p} = 1$, then $c_{i,q} = 0$, for $q \neq p$;

(2) if $c_{i,p} = 1$, then $c_{i-1,q} = 0$, for $q > p$;

Rule (1) indicates that the transmitting signal frequency of the n-th antenna in the k-th sub-chip can be any of the N frequencies in $\boldsymbol{F}_{\mathbf{set}}$. Rule (2) constrains the frequencies represented by $\boldsymbol{F}_k$ in an ascending sort order.

Obviously, each SFM matrix $\boldsymbol{C}_k$ corresponds to a certain binary data sequence to be modulated. The information modulation procedure corresponding to (3) is shown in Fig. 3(a). Essentially, information is modulated by utilizing the different frequencies and the corresponding transmitting antenna numbers. For one entire transmit pulse, the two-dimension frequency matrix $\boldsymbol{F}$ is shown in Fig. 3(b). Eventually, at the receiver, the transmitting space specialty is turned into amplitude modulation on frequencies.

As aforementioned in (3), there is a one-to-one mapping between each SFM matrix $\boldsymbol{C}_k$ and a certain bits binary data. Assuming that set $\boldsymbol{C}$ contains all the optional $\boldsymbol{C}_k$ within the constraints of rules (1) and (2). According to the relevant knowledge in information theory, the larger set $\boldsymbol{C}$ is, the higher entropy each $\boldsymbol{C}_k$ carriers. Thus, the data rate is positively related to the element number of set $\boldsymbol{C}$.

Let $Num(I, J)$ be the number of matrices $\boldsymbol{C}_k \in \mathbb{Z}^{I \times J}$ satisfying rules (1) and (2). We can obtain the following three equations after analyzing the characters of $\boldsymbol{C}_k$.

$$\begin{aligned} Num(2, J) &= \sum\nolimits_{j=1}^{J} j \\ Num(I, 2) &= I + 1 \\ Num(I, J) &= Num(I, J-1) + Num(I-1, J) \end{aligned} \tag{6}$$

$Num(N, N)$ can be calculated utilizing the recurrence relations above. Assume that the element of set $\boldsymbol{C}$ is presented by C_{num}, obviously, C_{num} is only related to the dimension of matrix $\boldsymbol{C}_k$. Clearly, the quantity of information each sub-chip carried is $\log_2 C_{num}$ and the data rate is $\eta \log_2 C_{num}/T_s$, where η is the duty cycle. The relation between antenna number N and data rate is shown in Fig. 4. We can see that the data rate

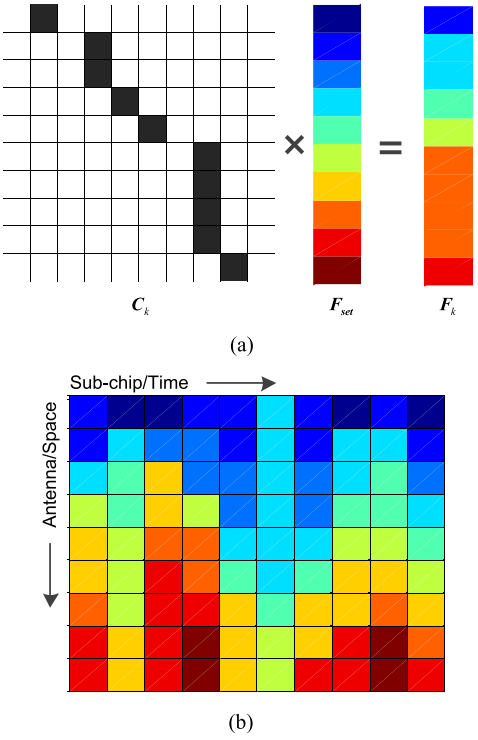

FIGURE 3. Schematic diagram of information modulation. (a) Modulation in one sub-chip. (b) An example of transmitting frequency matrix F for $N = N_a = 10, K = 10$.

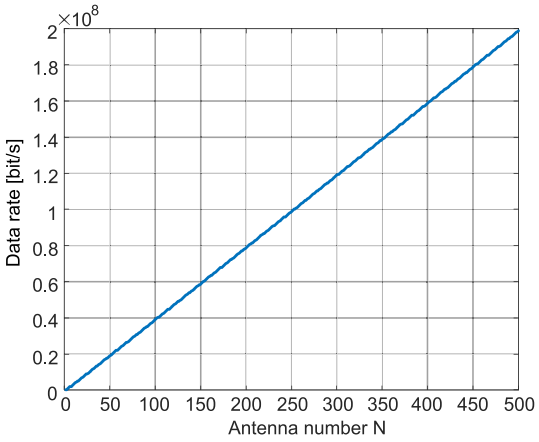

FIGURE 4. Data Rate for$\eta = 10\%$.

achieves million bits/s when $N > 25$ and is approximately linear with N.

For the communication function, transmitting information must be guaranteed to be accurate in the excepted direction. As has been stressed before, the relative power between different frequencies is crucial to the information demodulation. One of the most direct methods to preserve the relative power relationship is making it linear to the number of transmit antenna. Naturally, the beamforming technology is employed to meet that requirement. As the transmitting beamforming is exactly the conventional procedure used in a phased array radar system, the detailed derivation of the spatial synthesis of transmitted signals is omitted. After compensation of the initial phase related to antenna element position in the sub-array level, we can obtain the synthetic transmit signal at expected direction θ_c:

$$s_{\mathrm{T}}(t,\theta_c) = \sum_{k=1}^{K} \mathrm{rect}\left(\frac{t-(k-1)T_s-\tau}{T_s}\right) \boldsymbol{L}_k \boldsymbol{S}(t-(k-1)T_s-\tau) \tag{7}$$

$$\boldsymbol{L}_k = \begin{bmatrix} L_1 & L_2 & \cdots & L_N \end{bmatrix} = 1_N^{\mathrm{T}} \times \boldsymbol{C}_k. \tag{8}$$

$$\boldsymbol{S}(t) = \left[\exp\{j2\pi f_1 t\} \exp\{j2\pi f_2 t\} \quad \cdots \quad \exp\{j2\pi f_N t\}\right]^{\mathrm{H}} \tag{9}$$

C. ACF AND THE DRAWBACK

Regarding the radar function, the ACF of proposed SFM signal can be expressed as

$$R_{ACF}(\tau) = \int_{-\infty}^{+\infty} s_{\mathrm{T}}^*(t) s_{\mathrm{T}}(t-\tau)\, dt. \tag{10}$$

Transforming (7) and (10) to the frequency domain:

$$X(f) = \boldsymbol{\zeta}^{\mathrm{T}}(f)\boldsymbol{S}(f) \tag{11}$$

$$\chi_{ACF}(\tau) = \int_{-\infty}^{+\infty} X^*(f) X(f) \exp\{-j2\pi f\tau\}\, df \tag{12}$$

in which

$$\boldsymbol{\zeta}(f) = \boldsymbol{L}\boldsymbol{B}(f), \quad \boldsymbol{L} = [\boldsymbol{L}_1^{\mathrm{T}}\, \boldsymbol{L}_2^{\mathrm{T}} \cdots \boldsymbol{L}_K^{\mathrm{T}}] \tag{13}$$

$$\boldsymbol{B}(f) = \left[1 \exp\{-j2\pi f T_s\} \cdots \exp\{-j2\pi f(K-1)T_s\}\right]^{\mathrm{H}} \tag{14}$$

and

$$\boldsymbol{S}(f) = [T_s \mathrm{sinc}((f-f_1)T_s)\, T_s \mathrm{sinc}((f-f_2)T_s) \cdots T_s \mathrm{sinc}((f-f_N)T_s)]^{\mathrm{H}} \tag{15}$$

$\boldsymbol{B}(f)$ is the time steering of the transmitting signal corresponding to K sub-chips in time. $\boldsymbol{L}$ denotes the modulation result in the space-time domain. Hence, $\boldsymbol{\zeta}(f)$ represents the modulation both in space and time on each sub-band and shows the final effect on transmitting signal brought in by the information modulation. Fig. 5 gives the comparison of modulated and unmodulated ($K = 1$) sub-bands spectrum of transmitting signal. We can see the power distribution of sub-bands become fluctuant after modulation. The peak power of each sub-band is directly proportional to the total number of transmitting element allocated to the corresponding frequency. Besides, the inner spectrum of sub-band is also affected by time domain modulation.

Considering the orthogonality of different bands, the $\boldsymbol{\chi}_{ACF}$ can be rewritten as

$$\boldsymbol{\chi}_{ACF}(\tau) = \int_{-\infty}^{+\infty} \sum_{n=1}^{N} R_{\boldsymbol{\zeta}}^{n,n}(f) R_{\boldsymbol{S}}^{n,n}(f) \exp\{-j2\pi f\tau\} df \tag{16}$$

$$\boldsymbol{R}_{\boldsymbol{S}}(f) = \boldsymbol{S}(f)\boldsymbol{S}^H(f), \quad \boldsymbol{R}_{\boldsymbol{\zeta}}(f) = \boldsymbol{\zeta}(f)\boldsymbol{\zeta}^H(f) \tag{17}$$

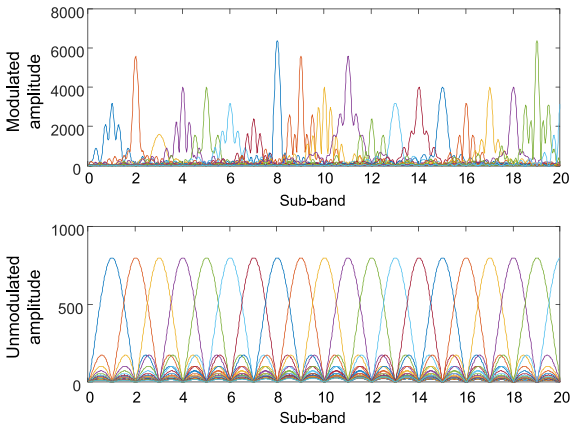

FIGURE 5. Frequency modulation for sub-bands.

From the equation above, $R_{\zeta}^{n,n}, n = 1, 2, \cdots, N$ reflects the final influence of space-frequency 2-dimension modulation on ACF. The effects of frequency spectrum modulation by $\boldsymbol{R}_{\boldsymbol{\zeta}}(f)$ are reflected in two aspects: 1) the non-uniform frequency spectrum brings in the unpredicted random sidelobes near the mainlobe; 2) the pulse width T_p is enlarged for each sub-band by the factor of K because of the arrangement of continuous K sub-chips in one pulse. With the frequency interval $\Delta f_s = 1/T_s = K/T_p$, the frequency sampling interval is K times larger for an unambiguous range profile. Thus, $2K-2$ grating lobes are symmetrically distributed with interval T_s.

III. MISMATCHED FILTER DESIGN

In the case of the radar operation, the additional modulated information is useless and even deteriorates the performance of target detection. Notice that the transmitting frequency matrix of each sub-chip can be utilized as prior information to remove the impact of spectrum modulation, which has been analysed in the previous section.

A. INFORMATION DEFUSION FOR RADAR OPERATION

Given that the bandwidth $B = N\Delta f_s \ll f_c$, frequency response of the reflect object is supposed to be flat over the whole band. Assuming that the Doppler frequency shift caused by relative movement can be ignored in one pulse, the signal part in received echo can be expressed briefly in frequency domain:

$$Y(f, \tau) = \rho \boldsymbol{\zeta}^{\mathrm{T}}(f)\boldsymbol{S}(f) \exp\{-j2\pi f\tau\}. \tag{18}$$

$\tau = 2r/c$ is the propagation delay corresponding to scattering distance r. c represents the speed of light. ρ is the complex coefficient including propagation attenuation, scattering frequency response and Doppler phase. Given the transmitting signal as (11), we can obtain the modulation result on the whole spectrum by a complex division.

$$M(f) = X(f)/S(f) = \frac{\boldsymbol{\zeta}^{\mathrm{T}}(f)\boldsymbol{S}(f)}{\mathbf{1}_N^{\mathrm{T}}\boldsymbol{S}(f)} \tag{19}$$

$S(f) = \mathbf{1}_N^{\mathrm{T}}\boldsymbol{S}(f, \theta)$ represents the unmodulated spectrum. Thus, the modulation on transmit signal can be removed by numerical operation to the received signal.

$$\tilde{Y}(f) = Y(f)/M(f) = \rho \mathbf{1}_N^{\mathrm{T}}\boldsymbol{S}(f) \exp\{-j2\pi f\tau\}. \tag{20}$$

Clearly, after preprocessing, the received signal is a standard orthogonal frequency division multiplexing (OFDM) signal without any data modulation. Amplitude modulation on transmit signal spectrum has been removed comparing with (11). Thus, the new MF corresponding filter to $\tilde{Y}(f)$ can be written as

$$\mathrm{H}_1(f) = \mathbf{1}_N^{\mathrm{T}}\boldsymbol{S}^*(f). \tag{21}$$

The entire processing procedure of received signal can be described as

$$\tilde{Y}(f)\mathrm{H}_1(f) = Y(f)\mathrm{H}_1(f)/M(f). \tag{22}$$

Considering the original received signal $Y(f)$ as input, the processes above are equal to a mismatched filter and the MMF can be expressed as

$$\mathrm{H}_{\mathrm{mis}}(f) = \frac{\mathrm{H}_1(f)}{M(f)} = \frac{\mathbf{1}_N^{\mathrm{T}}\boldsymbol{S}(f) \odot \left[\mathbf{1}_N^{\mathrm{T}}\boldsymbol{S}^*(f)\right]}{\boldsymbol{\zeta}^{\mathrm{T}}(f)\boldsymbol{S}(f)} \tag{23}$$

where $\odot$ denotes element-wise multiplication. The signal component in the output of the MMF can be given in the frequency domain as

$$\begin{aligned}\Theta(f) &= \tilde{Y}(f)\mathrm{H}_1(f) \\ &= \rho \exp\{-j2\pi f\tau\} \sum_{n=1}^{N} |T_s \mathrm{sinc}\left((f - f_n)\, T_s\right)|^2\end{aligned} \tag{24}$$

and the corresponding form in the time domain as

$$\chi(t) = \mathrm{IFFT}\{\Theta(f)\} = \rho \mathrm{tri}_{2T_s}(t-\tau)\frac{B}{2\pi}\mathrm{sinc}\left(B\left(t-\tau-nTs\right)\right). \tag{25}$$

From (24) and (25), we can see that, after information defusion, the PC result in the frequency domain is flat and the grating sidelobes are suppressed. More importantly, equation (25) shows that the PC result of different transmit pulse is coherent, which is crucial for clutter cancellation.

B. ANALYSIS OF SNR LOSS

MF theory gives the method of filter designing used to obtain the maximum output SNR in the background of white Gaussian noise. Compared with MF, the proposed MMF certainly results in SNR loss.

Considering the maximum SNR appears at certain time $t = T_{\mathrm{M}}$, the power of signal component is

$$|\chi(T_{\mathrm{M}})|^2 = \left| \int_{-\infty}^{\infty} Y(f)\mathrm{H}_{\mathrm{mis}}(f) \exp\{j2\pi f T_{\mathrm{M}}\}\, df \right|^2. \tag{26}$$

Assuming the interference is white noise with power spectral density $N_0/2$W/Hz, the noise power spectral density at the

output of receiver is $N_0/2\,|\mathrm{H_{mis}}(f)|^2$ W/Hz. The output noise power is

$$n_p = (N_0/2) \times \int_{-\infty}^{\infty} |\mathrm{H_{mis}}(f)|^2\, df. \tag{27}$$

The output SNR at $t = T_\mathrm{M} = \tau$ is

$$\mathrm{S/N_{mis}} = |\chi(T_\mathrm{M})|^2 / n_p. \tag{28}$$

When $\mathrm{H_{mis}}(f) = Y^*(f)$, we can obtain the maximum output SNR

$$\mathrm{S/N} = (2/N_0) \times \int_{-\infty}^{\infty} |Y(f,\theta)|^2\, df. \tag{29}$$

Thus, the SNR loss of MMF can be obtained by

$$\begin{aligned} SNR_\mathrm{loss} &= 10\log\left(\frac{\mathrm{S/N_{mis}}}{\mathrm{S/N}}\right) \\ &= 10\log\left(\frac{\left|\int_{-\infty}^{\infty} Y(f)\mathrm{H_{mis}}(f)\exp\{j2\pi f T_\mathrm{M}\}\,df\right|^2}{\int_{-\infty}^{\infty}|Y(f,\theta)|^2\,df \int_{-\infty}^{\infty}|\mathrm{H_{mis}}(f,\theta)|^2\,df}\right). \end{aligned} \tag{30}$$

C. FREQUENCY SPECTRUM MODIFICATION

In practice, the information defusion operation in (19) cannot be achieved in a system. The most problematic issue is the division operation may produce extra high response in MMF when $M(f)$ approaches zero. However, the near-zero modulation proves that the radiant energy at the corresponding frequency component is almost zero, i.e., the received data is approximately pure noise. The appearance of near-zero modulation can be ascribed to two reasons. One reason is the overlying of adjacent nonzero modulated sub-bands that appears between the centers of the sub-bands. The other reason is the original missing parts in the transmit spectrum caused by zero modulation that appears at the center of the sub-band.

From the previous analysis, it is the near-zero modulation that leads to the SNR loss. As one simple way to restrict the SNR loss to an acceptable level, we partly modified the MMF spectrum by utilizing the maximum SNR principle in the area of near-zero modulation.

Let α denote the decision threshold of near-zero modulation. Thus, the $M(f)$ is modified beforehand by

$$\begin{aligned} &\Psi : \{f\,|M(f) < \alpha\} \\ &\underset{f\in\Psi}{\hat{M}}(f) = 1/M(f), \end{aligned} \tag{31}$$

in which Ψ denotes the frequency set of near-zero modulation, and $\hat{M}(f)$ is the modified modulation response. As a result, $\mathrm{H_{mis}}$ can be rewritten as

$$\mathrm{H_{mis}}(f) = \begin{cases} \mathrm{H}_1(f)/M(f) & f \in \Psi \\ \mathrm{H}_1(f)M(f) & f \in \bar{\Psi}. \end{cases} \tag{32}$$

IV. SIMULATION RESULT

In this section, numerical simulation results are provided to illustrate the autocorrelation sidelobe characteristic and the effectiveness of the proposed MMF. The system parameters are listed in TABLE 1. Fig. 6 depicts the power spectral density (PSD) and the autocorrelation of the proposed waveform. From the experiment result, the range resolution of the SFM signal is the same as that of the unmodulated signal with the same bandwidth. However, the spectrum modulation introduced serious sidelobes in the autocorrelation that are not acceptable for the radar function. Fig. 7 shows the cross power spectral density (CPSD) and cross-correlation of the SFM signal and the corresponding MMF as described in (32). The sidelobes in the cross-correlation of the SFM pulse and MMF are found to be significantly suppressed and approximately consistent with what one would expect for an unmodulated waveform, except for the slight disturbance far away from the mainlobe.

Essentially, the first step of information defusion in (22) is consistent with the inverse filter (IF), which has been widely used in the area of image reconstruction. As has been analyzed previously, the IF procedure is sensitive to noise when the PSD of the expected signal is fluctuant. As an improved method over traditional IF, Wiener invert filtering (WIF) [18] enhances the noise resistance by introducing an addition item related to SNR in the denominator. The expression of WIF is given as follows:

$$\mathrm{WIF}(f) = \frac{\mathrm{H}^*(f)}{|\mathrm{H}(f)|^2 + \kappa \bullet S_n(f)/S_s(f)} \tag{33}$$

TABLE 1. System parameters.

Carrier frequency F_c	10 GHz
Frequency step interval Δf_s	2 MHz
Antenna number N	20
Sub-chip number K	5
Bandwidth B	40 MHz
Sub-chip width T_s	0.5 μs
Time-width T_p	2.5 μs

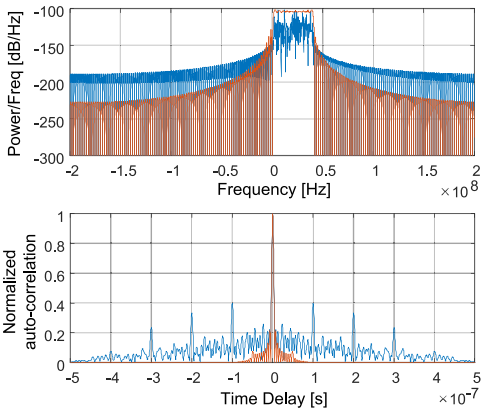

FIGURE 6. PSD/autocorrelation comparison of SFM signal (bule) and unmodulated signal (orange).

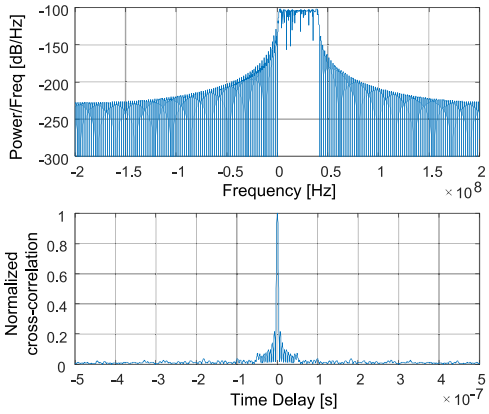

FIGURE 7. CPSD/cross-correlation of SFM signal and mismatched filter.

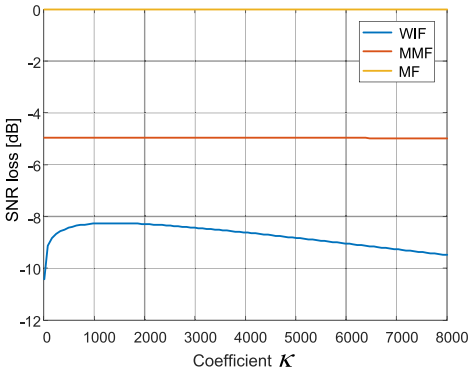

FIGURE 9. Processing SNR loss of WIF and the proposed MMF.

in which $S_n(f)$ and $S_s(f)$ represents the PSD of noise and signal respectively. κ is a constant coefficient.

Considering the target detection in noise background, the SNR is crucial to the detection performance. Here, we take the WIF as the method for performance comparison. Because the minimum modulation interval on sub-bands is one, we choose $\alpha = 1$ in (31). Regarding the WIF, the output SNR is influenced by the determination of coefficient κ. For a relative small κ, the modification on the filter caused by $\kappa \bullet S_n(f)/S_s(f)$ is limited. Thus, the signal power (SP) in the output of WIF maintains accordance with IF, whereas the amplification of noise power (NP) is reduced. On the contrary, for a relatively great κ, the amplification of noise can be well suppressed. However, the spectrum modification represented related to the addition item in the denominator also causes signal distortion and leads to SP loss.

First, 80 trials are conducted for κ from 1 to 8000 with the interval of 100 to find the optimal κ corresponding to minimum SNR loss. In each trial, the final result is obtained by taking the average value of 50 times repeated experiments. The resulting samples of WIF and MMF and the corresponding curves after 2-order nonlinear least squares fitting are shown in Fig. 8. Both SP and NP of WIF are found to decrease with the increasing of κ. The decreasing ratio of NP is greater than that of SP for κ from 1 to 1000, whereas the

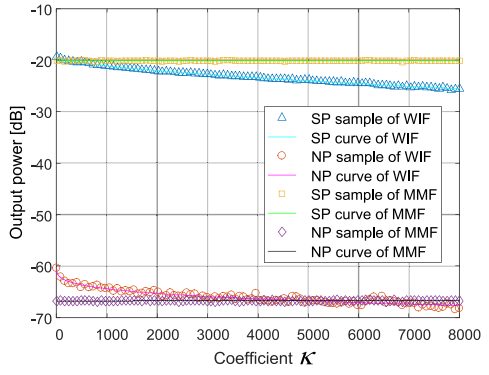

FIGURE 8. SP and NP in the output of WIF and proposed MMF.

opposite occurs from 2000 to 8000 evidently. Using the fitting result in Fig. 9, we can obtain the theoretical SNR loss of WIF and MMF. The result displayed is normalized by theoretical output SNR of MF. The SNR loss of MMF is less than 5 dB, which is still 3 dB lower than the minimum loss of WIF for κ from 1000 to 2000.

For radar modalities where clutter cancellation is required, it is important to maintain coherency over the set of M pulses within the coherent processing interval (CPI). The difference in the range responses sidelobe induces loss in Doppler coherency, thus limiting the efficacy of clutter cancellation. Compared with the IF output represented by (25), the spectral modification processes both in WIF and MMF, as given by (33) and (32), respectively, indeed realize SNR loss controlling at the expense of the loss of range sidelobe coherency. Let pulse number $M = 128$ in one CPI. The simulated model contains 853 range cells (from 1600 m to 1900 m) with the target placed in the center at a normalized Doppler shift of $+0.2$. The clutter cancellation is simply accomplished through deterministic Doppler filters produced by projection. The Doppler filter possesses a wide notch that also includes the 0 Doppler bin and the ± 2 Doppler bins to better suppress the Doppler-spread clutter. Figs. 10(a), (b) and (c) illustrate the difference in clutter cancellation performance for the IF, optimal WIF ($\kappa = 1500$) and proposed MMF, respectively, without regard to noise. The clutter to signal ratio (CSR) is 40 dB. In the absence of noise, we can clearly find that compared with optimal WIF and the proposed MMF, IF possesses better range sidelobe uniformity and thus less residual clutter in the output of Doppler filter. Although residual clutter is obvious in Fig. 10(c) for the current CSR, the target is still detectable with the amplitude being approximately 14 dB higher than the background residual clutter. However, for the optimal WIF, the target is totally undetectable. Consider the more realistic model with 10 dB SNR (after PC and Doppler processing) and 50 dB CNR after coherent integration. Figs. 10(d)-(f) illustrate the clutter cancellation performance for 3 filters. Compared with the proposed MMF, as shown in Fig. 10(c) and Fig. 10(f), the clutter cancellation performance of IF deteriorates sharply with the existence of noise. For the

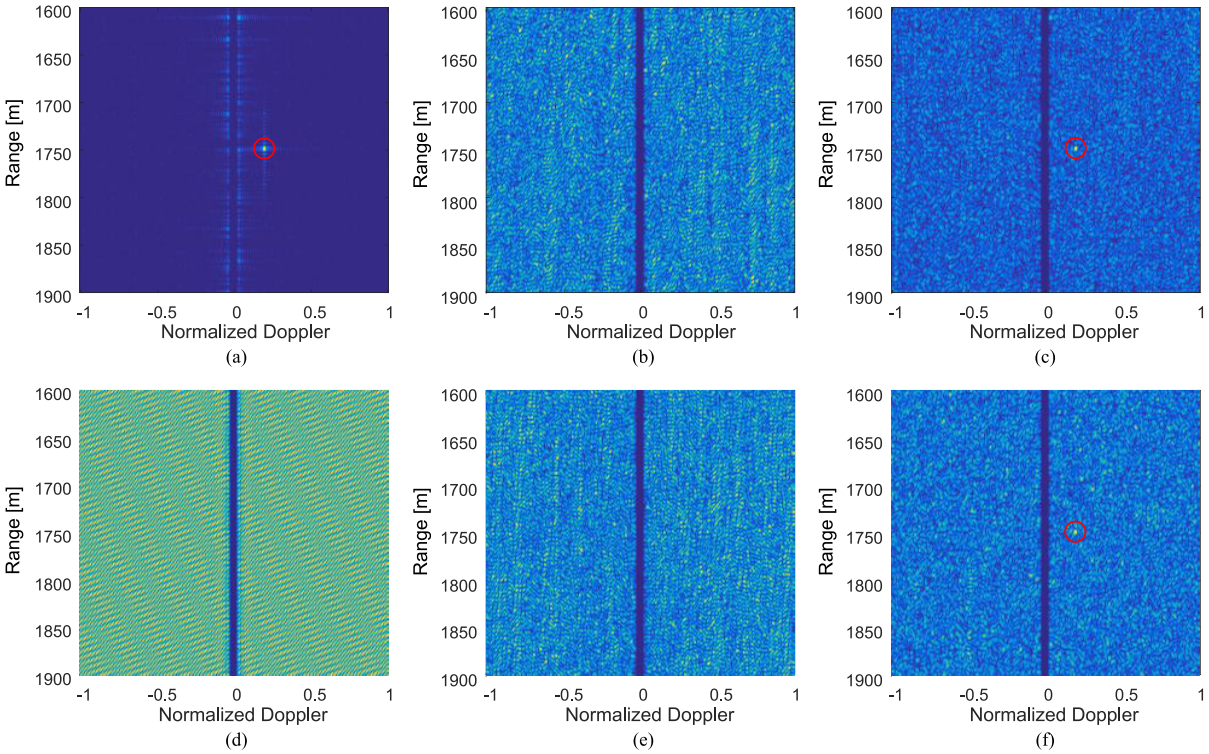

FIGURE 10. Comparison of range-Doppler processing using IF, WIF and MMF. (a) IF without noise; (b) WIF without noise; (c) MMF without noise; (d) IF with SNR = 10dB; (e) WIF with SNR = 10dB; (f) MMF with SNR = 10dB.

proposed MMF, the addition of noise indeed raises the background level. However, because of the good noise resistance of the proposed MMF, the target amplitude among noise and residual clutter is still in the detectable range, as shown in Fig. 10(f).

V. CONCLUSION

In this paper, we developed a space-frequency modulated co-design signal based on a multi-antenna system to serve radar and communication functions simultaneously. Specifically, the ACF performance deterioration caused by information modulation was analyzed. We proposed an IF based MMF to suppress ACF sidelobes that was proved to have less processing SNR loss than WIF through a simulation experiment. Furthermore, the subsequent Doppler processing of the proposed MMF between pulses in one CPI was assessed. The simulation results proved that the proposed co-design SFM radar-communication is feasible with regard to the basic radar signal processing.

REFERENCES

[1] G. C. Tavik *et al.*, "The advanced multifunction RF concept," *IEEE Trans. Microw. Theory Techn.*, vol. 53, no. 3, pp. 1009–1020, Mar. 2005.

[2] *Draft Supplement to Standard for Information Technology-Telecommunications and Information Exchange Between Systems-Local and Metropolitan Area Networks-Specific Requirements—Part 11: Wireless LAN Medium Access Control (MAC) and Physical Layer (PHY) SpecifiCations: Supplement to IEEE Std 802.11-1999*, IEEE Standard P802.11a/D7, 1999.

[3] L. Han and K. Wu, "24-GHz integrated radio and radar system capable of time-agile wireless communication and sensing," *IEEE Trans. Microw. Theory Techn.*, vol. 60, no. 3, pp. 619–631, Mar. 2012.

[4] S. C. Surender, R. M. Narayanan, and C. R. Das, "Performance analysis of communications & radar coexistence in a covert UWB OSA system," in *Proc. IEEE GLOBECOM*, Miami, FL, USA, Dec. 2010, pp. 1–5.

[5] M. Roberton and E. R. Brown, "Integrated radar and communications based on chirped spread-spectrum techniques," in *IEEE MTT-S Int. Microw. Symp. Dig.*, Philadelphia, PA, USA, Jun. 2003, pp. 611–614.

[6] G. N. Saddik, R. S. Singh, and E. R. Brown, "Ultra-wideband multifunctional communications/radar system," *IEEE Trans. Microw. Theory Techn.*, vol. 55, no. 7, pp. 1431–1437, Jul. 2007.

[7] X. Shaojian, C. Bing, and Z. Ping, "Radar-communication integration based on DSSS techniques," in *Proc. IEEE 8th Int. Conf. Signal Process.*, Beijing, China, Nov. 2006, pp. 1–4.

[8] C. Sturm and W. Wiesbeck, "Joint integration of digital beam-forming radar with communication," in *Proc. IET Int. Radar Conf.*, Guilin, China, Apr. 2009, pp. 1–4.

[9] M. J. Nowak, Z. Zhang, L. LoMonte, M. Wicks, and Z. Wu, "Mixed-modulated linear frequency modulated radar-communications," *IET Radar, Sonar Navigat.*, vol. 11, no. 2, pp. 313–320, 2016.

[10] S. Sen, "OFDM radar space-time adaptive processing by exploiting spatio-temporal sparsity," *IEEE Trans. Signal Process.*, vol. 61, no. 1, pp. 118–130, Jan. 2013.

[11] T. X. Zhang and X.-G. Xia, "OFDM synthetic aperture radar imaging with sufficient cyclic prefix," *IEEE Trans. Geosci. Remote Sens.*, vol. 53, no. 1, pp. 394–404, Jan. 2015.

[12] S. Sen and A. Nehorai, "Adaptive OFDM radar for target detection in multipath scenarios," *IEEE Trans. Signal Process.*, vol. 59, no. 1, pp. 78–90, Jan. 2011.

[13] C. Sturm and W. Wiesbeck, "Waveform design and signal processing aspects for fusion of wireless communications and radar sensing," *Proc. IEEE*, vol. 99, no. 7, pp. 1236–1259, Jul. 2011.

[14] C. Sturm, T. Zwick, and W. Wiesbeck, "An OFDM system concept for joint radar and communications operations," in *Proc. IEEE 69th Veh. Technol. Conf.*, Barcelona, Spain, Apr. 2009, pp. 1–5.

[15] C. Sturm, E. Pancera, T. Zwick, and W. Wiesbeck, "A novel approach to OFDM radar processing," in *Proc. IEEE Radar Conf.*, Pasadena, CA, USA, May 2009, pp. 1–4.
[16] A. Lozano, F. R. Farrokhi, and R. A. Valenzuela, "Lifting the limits on high speed wireless data access using antenna arrays," *IEEE Commun. Mag.*, vol. 39, no. 9, pp. 156–162, Sep. 2001.
[17] Z. Wang, G. Liao, and Z. Yang, "A novel radar waveform based on space-frequency coding compatible with directional communication," in *Proc. Int. Conf. RADAR*, Guangzhou, China, Oct. 2016, pp. 1–5.
[18] Y. Murayama and A. Ide-Ektessabi, "Bayesian image superresolution for hyperspectral image reconstruction," *Proc. SPIE*, vol. 8296, p. 829614, Feb. 2012.

ZHAOFENG WANG was born in Luoyang, Henan, China, in 1990. He received the B.S. degree in information engineering from Xidian University, Xi'an, China, in 2013.

He is currently pursuing the Ph.D. degree with the National Laboratory of Radar Signal Processing, Xidian University. His research interests include integrated waveform design and array radar signal processing.

GUISHENG LIAO (M'96–SM'16) was born in Guilin, Guangxi, China, in 1963. He received the B.S. degree from Guangxi University, China, in 1985, and the M.S. and Ph.D. degrees from Xidian University, Xi'an, China, in 1990 and 1992, respectively.

He is currently a Professor with the National Laboratory of Radar Signal Processing, Xidian University. He is also a Senior Visiting Scholar with The Chinese University of Hong Kong, Hong Kong. His research interests include array signal processing, space-time adaptive processing, synthetic aperture radar (SAR) ground moving target indication, and distributed small satellite SAR system design. He was a recipient of the National Outstanding Person Award in 2008 and the Cheung Kong Scholar Award in China in 2009.

ZHIWEI YANG was born in Nanchong, Sichuan, China, in 1980. He received the M.S. and Ph.D. degrees in electrical engineering from Xidian University, Xi'an, China, in 2005 and 2008, respectively. He is currently an Associate Professor with the National Laboratory of Radar Signal Processing, Xidian University. He designed the ground moving target indication algorithms for the space-borne synthetic aperture radar/ground moving target indication systems in China. His current research interests include adaptive array signal processing and space-time-polarimetric adaptive processing.